Synthesis and functionalization of iron oxide nanoparticles for targeted cancer therapy

Guillem Gabarró Riera

Supervisors: Dr Eva Carolina Sañudo[1,3], Dr Carlos Ciudad[2,3].
[1]Section of Inorganic Chemistry, Department of Inorganic Chemistry and Organic Chemistry, Faculty of Chemistry, University of Barcelona.
[2]Section of Biochemistry, Department of Biochemistry and Physiology, Faculty of Pharmacy, University of Barcelona
[3]Institute of Nanoscience and Nanotechnology University of Barcelona IN2UB

***Abstract*— Over the last decades, nanoparticles as drug carriers have attracted a lot of attention as potential systems for targeted drug delivery. Their tunable size and properties have opened a wide variety of possibilities to design future drug vehicles.**
On the other hand, Polypurine Reverse Hoogsteen Hairpins (PPRHs) molecules are DNA hairpins bound via Hoogsteen bonds. The PPRHs can bind by Watson-Crick bonds to the desired DNA sequence. In this particular case, the PPRHs are synthetized to act against the survivin production, which is an antiapoptotic protein, so its inhibition provokes cellular apoptosis, as it has already been proved and reported in literature.
In this work, a new system for targeted cancer therapy is presented from the combination of superparamagnetic iron oxide nanoparticles (SPIONs) and the PPRHs. Monodisperse SPIONs are synthetized and functionalized with dopamine, hyaluronic acid and PPRHs. Dopamine acts as an anchor to the nanoparticle, whereas hyaluronic acid is a known ligand to the CD44 receptor, apart from preventing the SPIONs to agglomerate. The paramagnetic behavior of these nanoparticles, along with their tunable size, makes them a very promising system for future cancer treatments.

***Index Terms*— 3. Nanopharmaceutics and Nanomedicine (*NanoPharmaMed*): cancer, nanoparticles, drug delivery, targeting.**

I. Introduction

Nanotechnology has had a dramatic impact on how scientists see and study the world. Among many different fields that have been affected by nanotechnology, medicine is one of the most promising: new drug synthesis, or just new ways to deliver already commercialized ones, are the hot topics in a brand-new field called nanomedicine [1].
Targeting is the term referred to the action of taking something directly to the place of interest. This phenomenon can be extremely relevant for many diseases such as cancer [2], where drug could be taken directly to the tumoral tissue. It is well-known that currently used treatments have several side effects due to the drug effect throughout the body, even on the healthy parts. The objective of targeting is to eliminate all the side effects by making the drug to act only on the pathological site. To do so, an appropriate vehicle must be properly designed, synthesized and tested. Targeting can be done passively, or actively. One example of the former is that nanosized entities are thought to be able to accumulate in tumoral tissues due to the so-called Enhanced Permeability and Retention effect (EPR), that originates from the bigger fenestrations in the blood vessels surrounding the tumor, allowing the entrance of objects that do not enter in healthy tissues [3]. Although the idea sounds incredibly good, it is necessary to consider another major factor when preparing a drug carrier: the environment inside a living organism is very challenging and hostile, and therefore rigorous attention must be paid to the different circumstances that could potentially alter the morphology and/or composition of the carrier.
Taking all the above-mentioned into account, there are many different systems that could be viable as drug nanocarriers, e.g. dendrimers, nanoparticles, nanotubes, vesicles, etc. [4].
In this work, the selected carriers have been magnetite (Fe_3O_4) nanoparticles due to their ease of synthesis, their ability to be functionalized with different compounds and also because of their superparamagnetic behavior [5]. From a pharmaceutical point of view, the drug carriers must have one particular property: they must have the same dimensions, this is, be monodisperse. For this reason, the synthetic route that has been followed is obtention of iron oxide nanoparticles coated with a monolayer of oleate. This synthetic route results in water insoluble nanoparticles, typically dispersed in chloroform, that are stable and present monodispersed sizes ranging from 10-20 nm depending on the experimental conditions [6], [7].
The superparamagnetic behavior is also an interesting property, since it could be used to drive the nanoparticles throughout the body towards the pathological site by using an external magnetic field (an example of active targeting), or because upon accumulation, hyperthermia could be produced by an AC magnetic field, and thus destroying the desired tissue. Another advantage of this magnetism is the possibility to enhance contrast in magnetic resonance imaging (MRI), as it has been reported in literature [8].
However, bare nanoparticles cannot be used directly to living organisms. They must be biocompatible and biodegradable, and for this reason many opt for coating them with different molecules.
One of the approaches scientists have carried out during the last years is to functionalize their vehicles with different polymers, such as polyethylene glycol (PEG) [9] or polyethyleneimine (PEI) [10], among many others. It is worth mentioning that,

besides improving biocompatibility, some of these polymers can act as ligands to certain receptors present in the membrane of tumoral cells, which would provide an additional route of active targeting.

The design of the system and its functionalization must be done taking into consideration the structure of the active principle that has to be carried. In this work, the active principle are DNA molecules called PolyPurine Reverse Hoogsteen (PPRHs). These molecules consist of DNA hairpins bound by reverse Hoogsteen bonds that, once inside the cell nucleus, bind to certain DNA sequence and inhibit the transcription factor. In this case, the PPRHs are designed to bind via Watson-Crick bonds to a DNA sequence that corresponds to the formation of a protein called *survivin*. This is an antiapoptotic protein, so its inhibition results in cell apoptosis, as it has been reported in literature [11]. However, it is reported that PPRHs cannot enter inside the cell by themselves, so a carrier is needed to transport them throughout the body and also through the cell membrane. The interaction between the carrier and the active principle must be moderate. If the interaction is strong, like covalent bonding, the active principle will not be released, and no therapeutic effect will be observed. On the other hand, if the interaction is very weak, the active principle will be lost before reaching the pathological site. For this reason, non-covalent interactions as hydrogen bonds or electrostatic interactions are attractive for binding the drug to the nanoparticle.

In this project, considering that the active principle, as a DNA molecule, has many different regions where these non-covalent interactions could be present, two systems have been proposed. The first one is a system consisting of the iron oxide nanoparticles (NPs) coated by a monolayer of dopamine (DA) and surrounded by hyaluronic acid (HA) and the PPRHs. While dopamine acts as an anchor, hyaluronic acid prevents the nanoparticles to agglomerate as well as it is a known ligand to the CD44 receptor which is present in the membrane of certain tumoral cells [12]. In this case, PPRHs are expected to be attached to the system by interactions like hydrogen bonds. The second system is a much simpler one, consisting only of the nanoparticles surrounded by the PPRHs. Iron oxide nanoparticles have positive charge on the surface, whereas PPRHs are negatively charged. Therefore, an electrostatic attraction is expected.

Characterization of the obtained systems is also a challenge due to their complex and organic structure. High-Resolution Transmission Electron Microscopy images are crucial to observe the system during the different synthetic steps. The employed microscope is equipped with an Energy Dispersive X-ray spectrometer to obtain a primary elemental analysis of the samples. However, TEM is not the most appropriate technique to observe organic matter, since the electron beam burns it immediately and therefore different spectroscopies have been performed to get a better understanding of the systems' composition.

This work presents a new approach to carry PPRHs throughout the body with the use of magnetite nanoparticles. With the aim to make the system biocompatible, organic molecules such as dopamine and hyaluronic acid are part of one of the proposed vehicles. Binding with bare nanoparticles and the PPRHs are also studied to investigate different possible vehicles for future works.

II. SYNTHESIS AND CHARACTERIZATION

Synthesis

All chemical compounds have been used as purchased.

A. Synthesis of Iron Oleate complex:

The iron oleate complex was synthetized using a modification of a procedure reported elsewhere [6]. 3.38 g of $FeCl_3 \cdot 6H_2O$ (Sigma-Aldrich, >99%) were dissolved in 12 ml of distilled water. The mixture was filtered, and the solution was added to a round bottom flask along with 10.98 g of sodium oleate (TCI Chemicals, >97%) , 42 ml of hexane (Panreac, 95%) and 24 ml of ethanol absolute (Panreac). The sample was heated up to 70 ºC for 4 hours under stirring and nitrogen atmosphere. The resultant product was a red-brownish solution which was separated and cleaned three times with distilled water. The solution was put in a rotary evaporator to eliminate the remaining hexane. The sample was kept under vacuum for 72 hours and then under nitrogen atmosphere for 23 hours. The resultant product was a red-brownish viscous oil that was preserved under nitrogen and without light exposure for future experiments.

B. Synthesis of oleate-coated iron oxide nanoparticles

Iron oxide nanoparticles coated with oleate groups were synthetized following a modified procedure reported in literature [6], [7]. In a typical experiment, 2.78 g of iron oleate (3 mmol) were added to a three-neck round bottom flask with 10 ml of eicosane (Sigma-Aldrich, 99%) and 0.96 ml of oleic acid (Sigma-Aldrich, >99%). The mixture was heated up to 95 ºC approximately and left at that temperature for a couple of minutes. Then, the sample was constantly heated up to 355 ºC at 3,3 ºC/min rate approximately under vigorous stirring and under reflux. Once the sample reached the desired temperature, the blackish mixture was cooled down to 50 ºC while keeping the reflux for three more minutes. 40 ml of acetone and 10 ml of hexane were added to the flask in order to precipitate the iron oxide nanoparticles. The sample was cleaned repeatedly with an acetone and hexane (4:1 volume) solution. The obtained nanoparticles were kept in different vials and dispersed in chloroform. Ethanol was used in one of the vials instead of chloroform to test the nanoparticles stability in this solvent.

C. Synthesis of dopamine-hyaluronic acid (DA-HA) adduct

201 mg of sodium hyaluronate (177kDa) were dissolved in 20 ml of distilled water (pH at 5.3). Then, 95.4 mg of dopamine hydrochloride (Sigma-Aldrich, 98%) and 81 mg of EDC (N-(3-Dimethylaminopropyl)-N'-(ethylcarbodiimide hydrochloride; Sigma-Aldrich) were introduced into the solution and the pH increased to 6.6. A drop of HCl 1M was added to reduce the pH down to 4-5. The sample was kept under stirring and HCl 1M drops were added to control the pH during the reaction. Once the pH did not increase, the reaction was finished.

D. PolyPurine Reverse Hogsteen (PPRHs) molecules

Coding-PPRHs, provided by the group of Dr Carlos Ciudad, were used in these experiments. To find polypyrimidine sequences in the target gene, Triplex-Forming Oligonucleotide Target Sequence Search software (http://utw10685.utweb.utexas.edu/tfo/) was used. BLAST

analyses were performed to confirm specificity of the designed PPRH without unintended targets.
The PPRH was synthesized as non-modified oligodeoxynucleotide by Sigma-Aldrich (Madrid, Spain) (0.05 mmol scale). The lyophilized PPRH was resuspended in sterile Tris-EDTA buffer (1 mM EDTA and 10 mM Tris, pH 8.0; AppliChem, Barcelona, Spain) and stored at -20 ºC.

E. Formation of the system NPs-PPRHs

200 µl of oleate-coated iron oxide nanoparticles in chloroform (5 mg/ml) were mixed with 200 µl of a solution of PPRHs 100 nM. The samples were left shaking for 72 hours. The aqueous phase containing the system NPs-PPRHs was separated with a micropipette and saved in a vial.

F. Formation of the system NPs-DA-HA

The same volume of NPs-Oleate and DA-HA adduct were mixed and left at the shaker for 72h approximately to ensure the maximum ligand exchanging. The black aqueous solution was separated using a micropipette and preserved covered from light and in the fridge.

G. Formation of the system NPs-DA-HA-PPRHs

20 µl of the NPs-DA-HA solution were mixed with 0.33 ml of PPRHs 100 nM solution. The mixture was left at the shaker for 72h approximately. After that period, the sample was left covered from light and saved in a fridge at 5ºC.

Characterization

The oleate-coated iron oxide nanoparticles (NPs-Oleate) and the systems NPs-PPRHs, NPs-DA-HA and NPs-DA-HA-PPRHs were characterized at the Serveis Cientifico-tècnics of the University of Barcelona (CCiTUB) using a JEOL J2100 (LaB6 filament) Transmission Electron Microscope (USA) operating at 200 kV equipped with a GATAN digital camera (Gatan Inc., Pleasaton, CA, USA). To analyze and process high-resolution TEM (HR-TEM) images, Gatan Digital Micrograph software was used.
Elemental analysis was also performed inside the microscope with an INCA x-sight spectrometer from Oxford Instruments, with Si (Li) detector. Spectra acquisition was accomplished using the INCA Microanalysis Suite version 4.09 software.
To characterize different samples like the adduct dopamine-hyaluronic acid (DA-HA), UV-Vis spectroscopies were carried out. The used spectrophotometer is a UV-Vis Cary 100 Scan 388 Varian using a 1 cm path length quartz cuvette. The absorption spectra were recorded on Perkin Elmer LAMBDA 950 UV-Vis spectrophotometer.
IR spectra were collected in a FT-IR Thermo Scientific Nicolet™ iS5 Spectrometer equipped with an iD7 ATR accessory.
Fluorometry experiments were performed in a Near-IR Spectrofluorometer for Nanotechnology from *HORIBA Jobin Yvon* with a 450 W intense broadband cw xenon lamp and iHR320 emission spectrograph. Spectra were collected by *Fluorescence* computer software from *HORIBA Jobin Yvon.*
In order to test the binding of PPRHs and the nanoparticles, electrophoretic experiments were carried out by the group of Dr Carlos Ciudad. The employed gel was composed by agarose (0.8%) and TAE buffer (Tris base, acetic acid and EDTA). Experiments were performed for approximately 2-3 hours at 10 V/cm at room temperature.

Cytotoxicity

The cytotoxicity experiments were carried out by the group of Dr Carlos Ciudad.

Cell culture

PC3 prostate adenocarcinoma cells (ECACC) were grown in Ham's F-12 medium supplemented with 7% fetal bovine serum (FBS, GIBCO, Invitrogen, Barcelona, Spain) and incubated at 37 ºC in a humidified 5% CO_2 atmosphere.

Transfection

Cells were plated in 35-mm-diameter dishes. The transfection procedure consisted in mixing the appropriate amount of PPRH and the different types of nanoparticles, using specific protocols described in the Results. As a positive control, the PPRH was also transfected with the cationic liposome N-[1-(2,3-dioleoyloxy)propyl]-N,N,N-trimethylammonium methylsulfate (DOTAP) (Roche, Barcelona, Spain) for 15 min at room temperature, followed by the addition of the mixture to the cells.

MTT assay

Cells were plated in 35-mm-diameter dishes in F12 medium. After 6 days, 0.63 mM of 3-(4,5-dimethylthiazol-2-yl)-2,5-diphenyltetrazolium bromide and 18.4 mM of sodium succinate (both from Sigma-Aldrich, Madrid, Spain) were added to the culture medium and incubated for 3 h at 37 8C. After incubation, the medium was removed and the solubilization reagent (0.57% acetic acid and 10% sodium dodecyl sulfate in dimethyl sulfoxide) (Sigma-Aldrich, Madrid, Spain) was added. Cell viability was measured at 570 nm in a WPA S2100 Diode Array spectrophotometer (Biochrom Ltd., Cambridge, UK).

III. RESULTS AND DISCUSSION

A. NPs-Oleate

Superparamagnetic iron oxide nanoparticles coated with a monolayer of oleate were synthetized following a procedure published elsewhere [6], [7]. As it is reported, following this synthetic route one can obtain nanoparticles with different sizes depending on the thermal treatment. In Fig. 1, the results from this synthesis are shown. Iron oxide nanoparticles were successfully synthesized, with an average size of 15.1 ± 0.8 nm. The as-obtained nanoparticles were dispersed in chloroform, where they remain stable for at least several months. This is the system from which the synthesis of the vehicles for the PPRHs start. To test stability in different solvents, NPs-Oleate were dispersed in a vial containing ethanol, but agglomeration of NPs formed rapidly and therefore this solution was discarded.

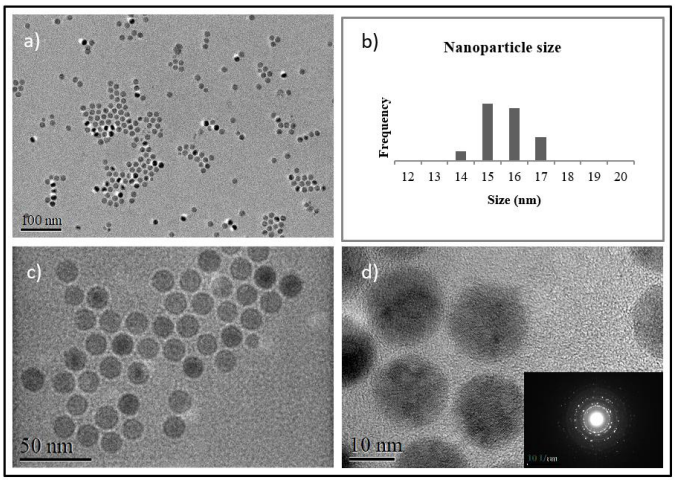

Fig. 1. *Iron oxide nanoparticles coated with a monolayer of oleate. a) and c) HR-TEM image of the NPs. b) Size distribution of the obtained nanoparticles. d) HR-TEM image of the NPs with the corresponding diffraction pattern, showing the crystallinity of the oleate-coated nanoparticles.*

B. Dopamine-Hyaluronic acid (DA-HA) adduct

As already mentioned before, biocompatibility is crucial when preparing new medicines. For this reason, the agglomeration of Fe_3O_4 nanoparticles inside the organism is something that must be avoided at all cost. By functionalizing the nanoparticles surfaces with organic molecules, the possible interaction between the magnetite nanoparticles can be suppressed. Nevertheless, this surface functionalization is also relevant to immobilize other molecules, e.g. the active principle or ligands to certain receptors to make the nanoparticle to target specific sites. Given the aforementioned, dopamine (DA) and hyaluronic acid (HA) were the molecules selected to functionalize the surface of the iron oxide nanoparticles. As reported by spectroscopic studies by Chen and coworkers [13], dopamine is a bidentate enediol ligand that convert the under-coordinated Fe surface sites back to a bulk-like lattice structure with an octahedral geometry for iron, which may result in tight binding of DA to iron oxide.

To ensure that hyaluronic acid is also strongly bound to the dopamine and thus to the nanoparticle, an adduct between dopamine and hyaluronic acid has been prepared before adding them to the nanoparticle's solution. In order to do so, the synthetic procedure reported by Vismara, E. et al [14] has been followed. To form a covalent bond between the dopamine's amine group and the carboxylate from the hyaluronic acid, EDC (1-Ethyl-3-(3-dimethylaminopropyl) carbodiimide) was used as a base (Fig. 2).

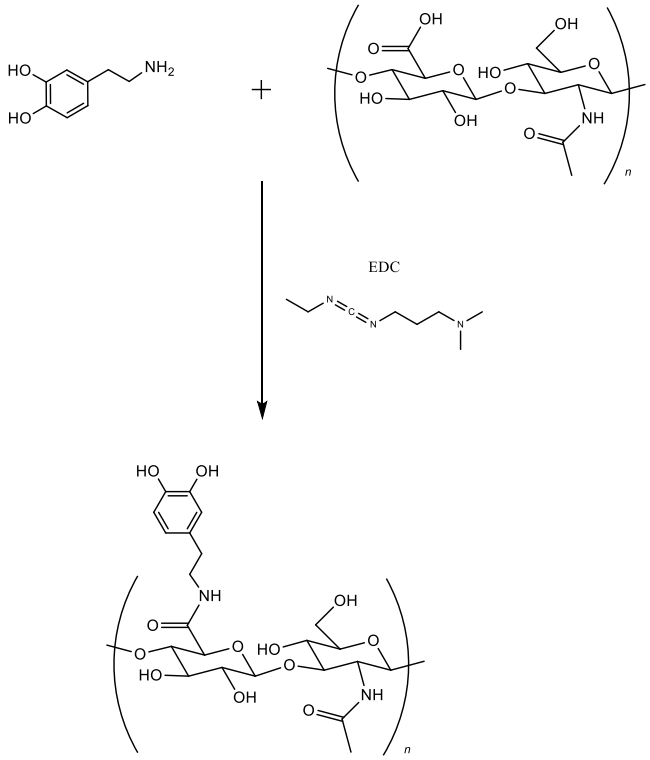

Fig. 2. *Reaction to produce the adduct dopamine-hyaluronic acid (DA-HA).*

The employed hyaluronic acid had a molecular weight of 177kDa, approximately. An excess of dopamine was added to ensure that all the carboxylate groups reacted, forming the corresponding amide.

The resultant product is a transparent aqueous solution that turns brownish with time. UV-Vis spectroscopy and IR spectroscopy techniques were performed to study the resultant product. As observed in Fig. 3 a), the UV-Vis spectrum presents two bands: one at ~275 nm and another at ~225 nm. Both bands coincide with those reported from the absorbance of dopamine [15].

To further characterize the obtained product, an infrared spectroscopy was performed. The solvent was evaporated using a rotary evaporator, resulting in a transparent greyish gel that was used to obtain the IR spectrum. In Fig. 3 b), it can be seen that the IR spectra from the DA-HA presents the typical bands from hyaluronic acid and dopamine [16]. Therefore, it is possible to say that the adduct was properly formed under the employed experimental conditions.

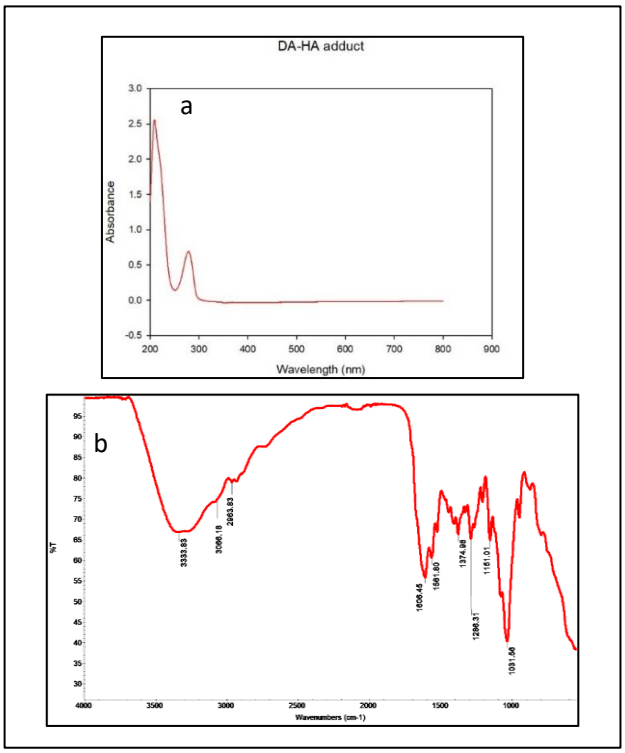

Fig. 3. *a) UV-Vis spectrum of the adduct DA-HA. b) IR spectrum of the obtained dopamine-hyaluronic acid adduct (DA-HA).*

C. NPs-DA-HA

To obtain the nanoparticles coated with dopamine and hyaluronic acid, a phase transfer was the method proposed. Oleate-coated nanoparticles are well dispersed in chloroform due to the monolayer of oleate that surrounds them. This solution was completely dark because of the presence of magnetite nanoparticles. On the other hand, the obtained DA-HA adduct was a transparent aqueous solution.

As dopamine binds strongly to the nanoparticle, when mixing the adduct with the NPs-Oleate solution, one could expect a ligand exchange between the oleate chains and the DA-HA compound. When mixing both solutions, the phase separation was clearly observed: the dark organic phase at the bottom containing the nanoparticles and the transparent aqueous phase above of it, containing the adduct. After mixing for 72 hours approximately in a shaker, the aqueous phase had turned black, indicating the presence of water-soluble iron oxide nanoparticles. By extraction with a micropipette, the aqueous phase was successfully separated and saved in a vial covered from light.

In order to characterize the new water-soluble nanoparticles, several techniques were performed.

HR-TEM images in Fig. 4 a) & b) show that the iron oxide nanoparticles did not suffer from any change in terms of size and crystallinity. Moreover, it can be observed that they arrange in a drop-like structure, probably because of the interaction between the hyaluronic acid molecules that surround the nanoparticles. Energy dispersive X-ray spectrum (Fig. 4 c)) shows high amounts of carbon from the DA-HA adduct around the nanoparticles.

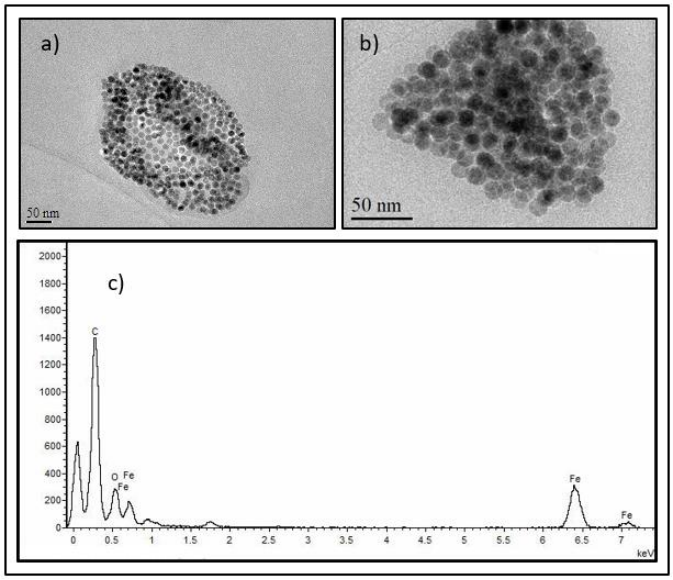

Fig. 4. *a) and b): HR-TEM images of the water-soluble NPs-DA-HA system. c) Energy Dispersive X-ray Spectroscopy spectrum from image b).*

It is worth mentioning that the solution of NPs-DA-HA is stable in water for more than a month, as no agglomeration is observed. On the contrary, the nanoparticles remain well dispersed in the medium, which is very important for new potential medicines using this kind of technology.

After evaporating the solvent using a rotary evaporator, the sample was a black gel because of the presence of water. Thermogravimetric analysis (TGA) was performed using this gel to try to quantify the mass percentage of the organic matter that surrounded the nanoparticles. In Fig. 5, the TGA results are represented. As it can be observed, at 100ºC approximately 11% of the total mass was lost. This is a clear indication that water was present in our sample, probably trapped by the hyaluronic acid network that formed around the nanoparticles. At temperatures between 144 ºC and 650ºC approximately, 55% of the total mass of the system was evaporated. This fact, along with the water solubility of the nanoparticles, evidence that oleate was no longer present around the NPs.

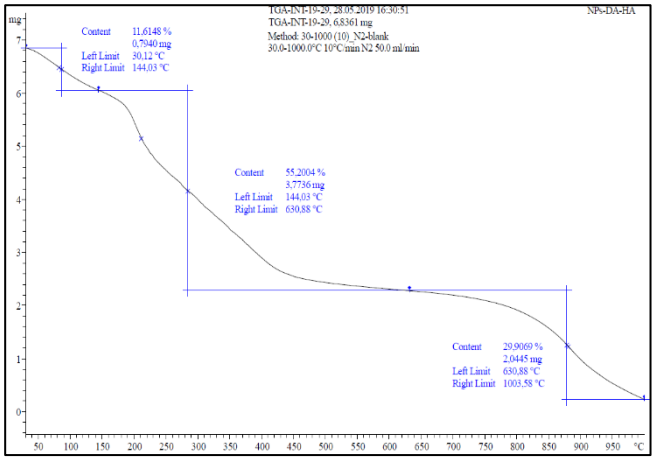

Fig. 5. *TGA results from the NPs-DA-HA system.*

Along with the stability shown by the nanoparticles in water, it is also interesting to mention that after evaporating the solvent, the gel-like sample was easily re-dispersed in MiliQ water, reiterating that the organic matter surrounding the nanoparticles was soluble in water.

D. NPs-DA-HA-PPRHs

Hyaluronic acid provides lots of sites where non-covalent interactions could eventually take place. Taking into consideration that PPRHs are DNA molecules, it is sensible to think that they would interact with the NPs-DA-HA. Therefore, just by mixing both products one could expect that some sort of binding would occur. PPRHs are negatively charged and are functionalized with fluorescein. For this reason, in a process like an electrophoresis, they run towards to positive pole and it is possible to observe this phenomenon with a fluorescent light. On the other hand, if these PPRHs are bound to the NPs, the overall charge of the system would be neutral and therefore would not move in the electrophoretic gel.
In order to test the amount of mixing time that is necessary to obtain a proper binding, an electrophoresis was performed. In Fig. 6, the results of the electrophoresis are depicted and clearly demonstrate that the mixing time and the amount of NPs were relevant in terms of PPRHs binding, as the amount of free PPRHs that ran through the gel decreased with larger mixing times and higher concentration of nanoparticles. The amount of PPRHs was the same in all samples (10 µl of a 10 µM solution). The first electrophoresis was performed at 5 ºC. To test also the effect of temperature in the mixing, a second electrophoresis was performed at room temperature (Fig. 7). After 72h of shaking a solution of NPs-DA-HA (10 mg/ml) and PPRHs 100 nM at room temperature, no free PPRHs were present.

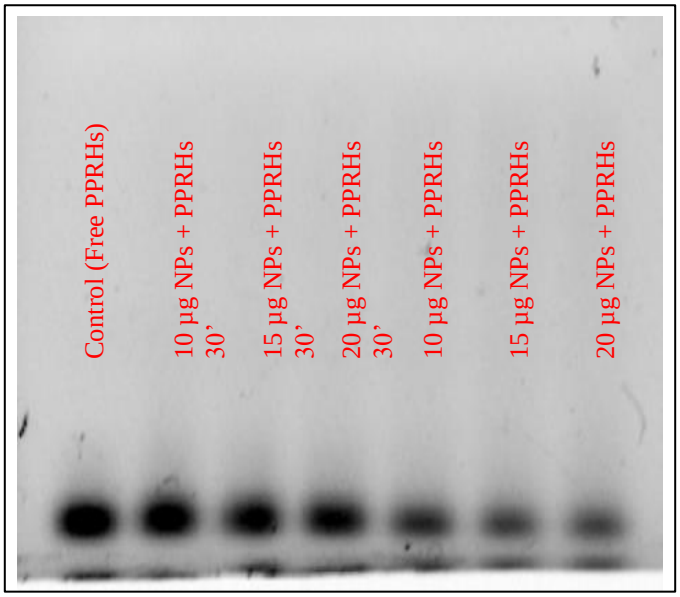

Fig. 6. *Electrophoresis with different mixing times and different amounts of NPs-DA-HA. The black area at the bottom represents the quantity of free PPRHs present in solution. As mixing time increased, the number of free PPRHs molecules decreased.*

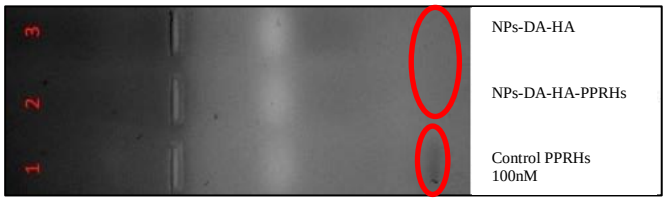

Fig. 7. *Electrophoresis demonstrating that no free PPRHs were present in solution after 72h of mixing at room temperature.*

HR-TEM images (Fig. 8) show nanoparticles surrounded by organic matter, similarly to those obtained in the NPs-DA-HA system. However, as PPRHs are DNA molecules, bases within the sequence are bound via phosphate groups. For this reason, if the organic matter observed in the TEM images contained PPRHs, phosphorous should be present in the Energy Dispersive X-ray (EDX) spectra. In Fig. 8, these TEM images are presented along with the corresponding EDX. As it can be observed, the nanoparticles present the same size than the first NPs-Oleate system (15 nm approximately) and they are also crystalline, illustrating that the magnetite core of the nanoparticles did not change during the functionalization processes.
Moreover, as expected, EDX shows the presence of phosphorous, indicating that the NPs-DA-HA-PPRHs system was successfully synthesized.
As commented before, PPRHs molecules are functionalized with fluorescein. If the organic matter that surrounded the nanoparticles observed in TEM images corresponded to polypurine molecules, they should have absorbed and emitted radiation due to the presence of fluorescein. In order to corroborate this, fluorimetry experiments were performed. So as to compare the effect of the concentration of fluorescein in the emission spectrum, highly and lowly concentrated solutions of fluorescein were measured, as well as the solution containing

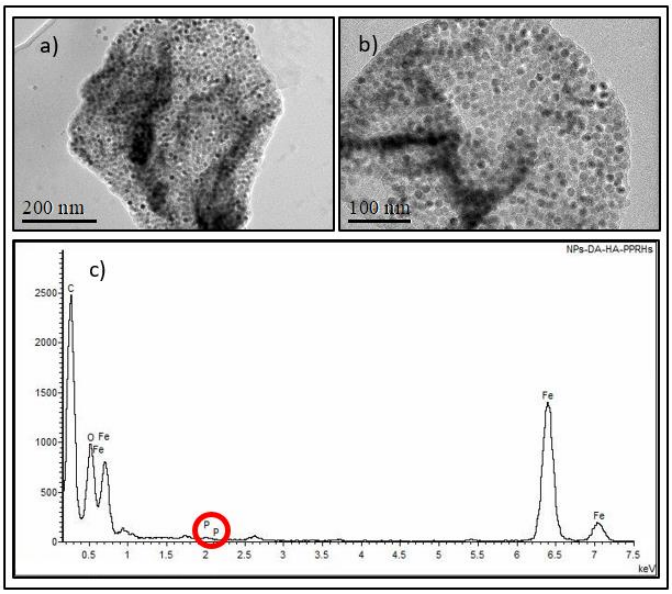

Fig. 8. *a) and b): HR-TEM images of the system NPs-DA-HA-PPRHs system. c) Energy Dispersive X-ray Spectroscopy spectrum from image a).The presence of phosphorous is a clear suggestion of the presence of PPRHs (red circle)*

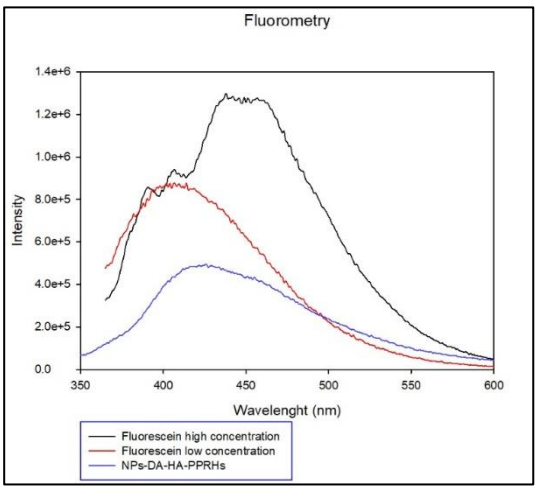

Fig. 9. *Fluorometry spectrum of different solutions of fluorescein and NPs-DA-HA-PPRHs*

the nanoparticles. The results in Fig. 9 show that the solution NPs-DA-HA-PPRHs presented fluorescence, at approximately the same wavelength than the fluorescein control samples, remarking thus that the functionalization had actually taken place.

E. Cytotoxicity of NPs-DA-HA-PPRHs

As previously mentioned, even though PPRHs produce cell apoptosis, they do no have the ability to enter inside the cell by themselves. For this reason, a decrease in cell viability could mean the presence of PPRHs inside the cell. For this reason and to further characterize the obtained system, preliminary cytotoxicity experiments were carried out in 10000 PC3 prostate adenocarcinoma cells.
In Fig. 10, results are shown. The employed experimental conditions were the ones that demonstrated to be the best ones in Fig. 6. The mixing time was 72h and the most adequate amount of nanoparticles was 20 µg. In this way, different

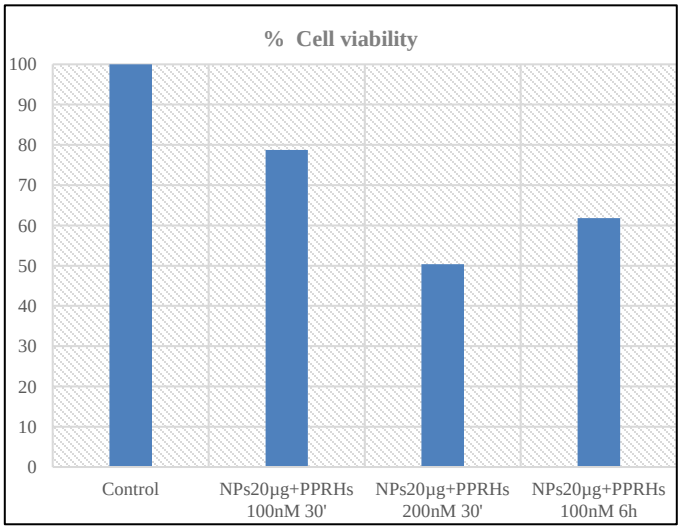

Fig. 10. *Viability assay results. Cell viability decreased when system NPs-DA-HA-PPRHs was introduced.*

transfection times (30 minutes and 6h) and different amount of PPRHs were studied (10 µl of 100 nM and 200 nM of PPRHs). Cell viability decreased and presented different values depending on the loading of PPRHs and on the transfection times. These results must not be misunderstood, as they are very preliminary, and more experiments should be made in order to obtain more data and to study the best experimental conditions.

F. NPs-PPRHs

Even though dopamine and hyaluronic acid provide the highly desired biocompatibility and the hindering of NPs agglomeration, it is also interesting to study whether the structure of the PPRHs is adequate to produce a ligand exchange with the oleate, that is, remove the oleate from the NPs-Oleate system and surround the nanoparticles with the PPRHs. Since the iron oxide nanoparticles have a positive charge density on their surface and the PPRHs are negatively charged, an electrostatic interaction could be expected.
A similar procedure to form the NPs-DA-HA was followed to try to obtain a system consisting of only nanoparticles and the polypurines. Same volumes of NPs-Oleate (10 mg/ml) and PPRHs solution (100 nM) were mixed and left shaking for several days at room temperature. The aqueous phase, transparent at the beginning of the experiment, turned whitish and turbulent. By phase separation with a micropipette, the aqueous phase was saved to analyze via TEM and EDX. In Fig. 11, the results are presented. Water-soluble iron oxide nanoparticles surrounded by PPRHs were present in solution, indicating that the system NPs-PPRHs was formed. Moreover, the nanoparticles were crystalline and monodisperse, indicating that they had not suffered from any change in terms of morphology and composition. It could also be possible that oleate was not removed from the surface of the nanoparticles, forming a hybrid system that consists of NPs-Oleate-PPRHs.

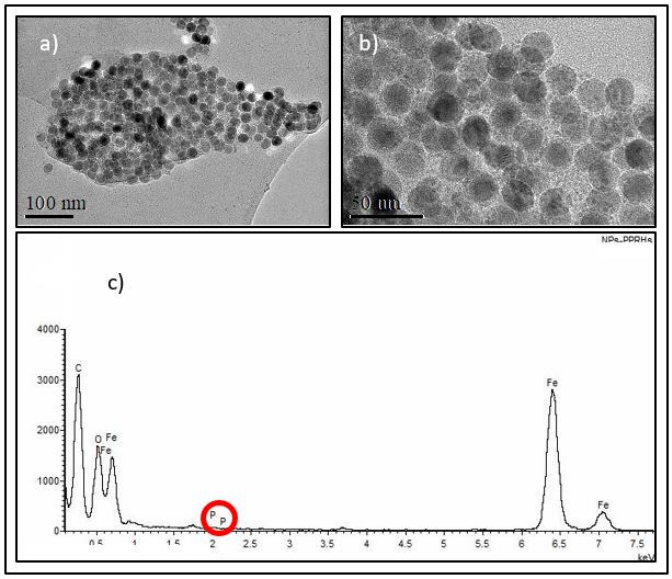

Fig. 11. *a) and b): HR-TEM images of the system NPs-PPRHs system. c) Energy Dispersive X-ray Spectroscopy spectrum from image a). As well as in the sample NPs-DA-HA-PPRHs, the presence of phosphorous is a good indicative of the presence of PPRHs.*

Further experiments should be performed to optimize the experimental conditions and to determine the real structure of the resultant system.

IV. CONCLUSIONS

The objectives of this work have been successfully achieved.
A vehicle for the PPRHs is essential to drive them towards the pathological site and to help them get inside the desired tissue. Two different vehicles have been designed, taking into consideration very important factors like biocompatibility and biodegradability, one consisting of nanoparticles, dopamine, hyaluronic acid and PPRHs, and the other consisting of nanoparticles and PPRHs. The synthetic procedures have also been a success, as demonstrated by different characterization techniques such as HR-TEM and different spectroscopies. With such functionalization, stable water-soluble nanoparticles have been obtained. Moreover, even not being in the scope of this work, preliminary cytotoxicity experiments were carried out, indicating that the system NPs-DA-HA-PPRHs decreases cell viability. The prospect of being able to obtain this kind of systems based on nanoparticles and PPRHs serves as a continuous spur to future research.

ACKNOWLEDGMENT

G.G. Author thanks supervisors Dr Eva Carolina Sañudo and Dr Carlos Ciudad for their help and support throughout the making of this work. Also, G.G. would like to thank Chiara, Erasmus student from Dr Ciudad's group, for her help in the different cellular studies and in the electrophoresis experiments. E.C.S. and G.G. acknowledge financial support from Spanish Government (Grant CTQ2015-68370-P).

REFERENCES

[1] Moghimi, S. M., Hunter, A. C. & Murray, J. C. Nanomedicine: current status and future prospects. *FASEB J.* **19**, 311–330 (2005).
[2] Jain, R. K. & Stylianopoulos, T. Delivering nanomedicine to solid tumors. *Nat. Rev. Clin. Oncol.* **7**, 653–664 (2010).
[3] Maeda, H., Wu, J., Sawa, T., Matsumura, Y. & Hori, K. Tumor vascular permeability and the EPR effect in macromolecular therapeutics: a review. *J. Control. Release* **65**, 271–284 (2000).
[4] Peer, D. *et al.* Nanocarriers as an emerging platform for cancer therapy. *Nat. Nanotechnol.* **2**, 751–760 (2007).
[5] Morales, D. M. P., Bo, I. B., Heverhagen, J. T., Prosperi, D. & Parak, W. J. Biological applications of magnetic nanoparticles. **41**, 4306–4334 (2012).
[6] Park, J. *et al.* Ultra-large-scale syntheses of monodisperse nanocrystals. *Nat. Mater.* **3**, 891–895 (2004). Sun, C., Lee, J., & Zhang, M. (2008).
[7] Bronstein, L. M. *et al.* Influence of Iron Oleate Complex Structure on Iron Oxide Nanoparticle Formation. *Chem. Mater.* **19**, 3624–3632 (2007).
[8] Sun, C., Lee, J. S. H. & Zhang, M. Magnetic nanoparticles in MR imaging and drug delivery. *Adv. Drug Deliv. Rev.* **60**, 1252–1265 (2008).
[9] Jokerst, J. V, Lobovkina, T., Zare, R. N. & Gambhir, S. S. Nanoparticle PEGylation for imaging and therapy Review. *Nanomedicine* **6**, 715–728 (2011).
[10] Li, J. *et al.* Biomaterials Hyaluronic acid-modified hydrothermally synthesized iron oxide nanoparticles for targeted tumor MR imaging. *Biomaterials* **35**, 3666–3677 (2014).
[11] Ciudad, C. J. & Villalobos, X. Polypurine Reverse Hoogsteen Hairpins as a Gene Silencing Tool for Cancer. *Curr. Med. Chem.* **24**, 2809–2826 (2017).
[12] Mattheolabakis, G. *et al.* Hyaluronic acid targeting of CD44 for cancer therapy: from receptor biology to nanomedicine Hyaluronic acid targeting of CD44 for cancer therapy: from receptor biology to nanomedicine. *J. Drug Target.* **23**, 605–618 (2015).
[13] Chen, L. X., Liu, T., Thurnauer, M. C., Csencsits, R. & Rajh, T. Fe2O3 Nanoparticle Structures Investigated by X-ray Absorption Near-Edge Structure, Surface Modifications, and Model Calculations. *J. Phys. Chem. B* **106**, 8539–8546 (2002).
[14] Vismara, E. *et al.* Superparamagnetic Iron Oxide Nanoparticles Loaded with Paclitaxel for Biomedical Applications. *Molecules* **22**, 1030/1-1030/25 (2017).
[15] Wei, Q., Zhang, Y. & Li, J. Preparation of Surface Molecularly Imprinted Poly (dopamine) Film for 4- Hydroxybenzoic Acid (4-BA) Recognition by One-Step Method. *Anal. Lett.* **44**, 1796–1806 (2011).
[16] Lih, E., Choi, S. G., Ahn, D. J., Joung, Y. K. & Han, D. K. Optimal conjugation of catechol group onto hyaluronic acid in coronary stent substrate coating for the prevention of restenosis. *J. Tissue Eng.* **7**, 1–11 (2016).